Palaeogeography, Palaeoclimatology, Palaeoecology 313-314 (2012) 70–77

Contents lists available at SciVerse ScienceDirect

Palaeogeography, Palaeoclimatology, Palaeoecology

journal homepage: www.elsevier.com/locate/palaeo

The skeletal geochemistry of the sclerosponge *Astrosclera willeyana*: Implications for biomineralisation processes and palaeoenvironmental reconstruction

Nicola Allison [a,*], Alexander W. Tudhope [b], EIMF [c]

[a] Department of Earth Sciences, University of St Andrews, Irvine Building, North Street, St Andrews, Fife KY16 9AL, UK
[b] School of Geosciences, University of Edinburgh, Edinburgh EH9 3JW, UK
[c] NERC Ion Microprobe Facility, Grant Institute, University of Edinburgh, Edinburgh EH9 3JW, UK

ARTICLE INFO

Article history:
Received 25 March 2011
Received in revised form 5 October 2011
Accepted 19 October 2011
Available online 26 October 2011

Keywords:
Sclerosponge
Sr/Ca
Mg/Ca
SST
SIMS
Astrosclera

ABSTRACT

To investigate the controls on the geochemistry of aragonitic sclerosponge skeletons, we used secondary ion mass spectrometry (SIMS) to analyse an *Astrosclera willeyana* specimen. The high spatial resolution of SIMS allows the independent analysis of the two key crystal structures in the skeleton i.e. the fused spherulites (formed intracellularly and fused together at the surface of the skeleton) and the epitaxial backfill (deposited extracellularly at the base of the sponge tissue). We analysed Sr/Ca, Mg/Ca and Ba/Ca across a short (~5 mm) transect of fused spherulites which represented several years growth. We observe cyclical variations (with a length of 0.1 to 0.6 mm in both Sr/Ca and Mg/Ca in some (but not all) sections of the transect. The observed ranges of Sr/Ca and Mg/Ca over the presumed seasonal cycles are ~9.5 to 11.5 mmol mol^{-1} and 0.6 to 1.0 mmol mol^{-1} respectively. The annual seawater temperature range at the study site is ~4.3 °C, so the inferred temperature sensitivity of skeletal Sr/Ca and Mg/Ca is ~0.5 mmol mol^{-1} °C (or 5%°C^{-1}) and ~0.1 mmol mol^{-1}°C (or 13%°C^{-1}) respectively. This is higher than observed in most previous sclerosponge studies or anticipated from studies of synthetic aragonite. This indicates that the chemistry of the *A. willeyana* skeleton is affected by one or more additional influences, besides temperature, which are currently unresolved. The pH of the precipitating fluid, estimated from skeletal $\delta^{11}B$, is ~8.1–8.2 for both fused spherulites and epitaxial backfill. Epitaxial backfill contains significantly higher Sr/Ca, Mg/Ca and B/Ca and significantly lower Ba/Ca than the fused spherulites but Sr/Ca and Mg/Ca are positively correlated by the same relationship in both skeletal features. This suggests that the geochemistry of each feature is predominantly controlled by a common process. This is unlikely to be Rayleigh fractionation, which is indicated by negative correlations between Sr and Mg in aragonite.

1. Introduction

The isotope and trace element chemistry of marine calcite and aragonite skeletons is used frequently to infer past environmental conditions. Sclerosponges are long-lived and their skeletons may provide archives of environmental conditions over periods of 100–1000 years. The Sr/Ca of synthetically precipitated aragonite is temperature dependent (e.g. Kinsman and Holland, 1969) and sclerosponge skeletal Sr/Ca may indicate seawater temperatures (e.g. Haase-Schramm et al., 2003). Seasonal variations in skeletal Sr/Ca and seawater temperature correlate well ($r^2 = 0.67$) in a specimen of the Caribbean sclerosponge, *Ceratoporella nicholsoni*, (Rosenheim et al., 2004) but less well ($r = \sim 0.5$) in specimens of the Indo-Pacific species, *Astrosclera willeyana* (Fallon et al., 2005).

Accurate calibration of the relationship between skeletal Sr/Ca and seawater temperature is complicated by the growth habit of sclerosponges. The sponge tissue occupies calicles in the outermost 0.5–1 mm of the skeleton in *C. nicholsoni* (Swart et al., 2002; Rosenheim et al., 2009) and ~5 mm in *A. willeyana* (Fallon et al., 2005). Skeletal deposition occurs both at the skeleton surface and towards the base of the calicle. Annual linear extension rates are 0.1–0.4 mm yr^{-1} for *C. nicholsoni* (Böhm et al., 1996, 2002; Swart et al., 2002) and 0.2–1.8 mm yr^{-1} for *A. willeyana* (Worheide 1998; Moore et al., 2000; Fallon and Guilderson 2005; Fallon et al., 2005; Grottoli et al., 2010). Consequently aragonite deposited at the base of the tissue layer serves to thicken and infill structures which may have been deposited up to several years previously and drilled or milled sampling horizons, cut parallel to the sponge surface, combine mixtures of materials of significantly different ages. In *C. nicholsoni* backfill is precipitated in the bottom quarter of the tissue layer and backfilled skeleton may consist of ~20% older calicle wall material, originally deposited at the skeleton surface, and ~80% younger backfill (Böhm et al., 1996). In contrast, in *A. willeyana*, skeletal density increases gradually over most of the depth of the tissue layer suggesting that backfilled skeleton represents material which has been deposited and thickened almost continuously (Fallon et al., 2005). Variations in the timing and relative placement of skeletal accretion may explain the different success of each species in recording seasonal seawater temperatures.

* Corresponding author. Fax: +44 1334 463949.
E-mail address: na9@st-andrews.ac.uk (N. Allison).

0031-0182/$ – see front matter © 2011 Elsevier B.V. All rights reserved.
doi:10.1016/j.palaeo.2011.10.009

The aragonite deposited at the skeleton surface consists of intracellularly formed spherulites which are fused by epitaxial growth while the aragonite deposited at the base of the tissue layer consists of epitaxial backfill which precipitates extracellularly. In *A. willeyana* the spherulites form within vacuoles inside mobile large vesicle cells in the ectosome, the upper tissue layer of the sponge (Worheide 1998). As the membrane of the large vesicle cell lyses (breaks down), the spherulite is released and subsequently enveloped by one or more basopinacocyte cells which have invaded the sponge tissue. The basopinacocytes transport the spherulites to the skeleton where they are attached to the vertically growing skeletal pillars. These spherulites are then fused by epitaxial processes. Epitaxial backfill is deposited at the base of the tissue layer as the sponge tissue is slowly drawn upwards, vacating the skeletal pore spaces. Any variation in Sr/Ca partitioning between the fused spherulites and the epitaxial backfill will complicate the Sr/Ca–seawater temperature relationship preserved in the skeleton.

To further investigate controls on the geochemistry of *A. willeyana* skeletons, we used secondary ion mass spectrometry (SIMS) to analyse a single skeleton at a high spatial resolution. We used a primary beam diameter of 15–35 μm allowing us to characterise the geochemistry of the different skeletal features i.e. the fused spherulites and epitaxial backfill. We analysed a transect, along the fused spherulites, perpendicular to the skeleton surface, to investigate if these features record any seasonal environmental signal. We determined Sr/Ca, Mg/Ca, Ba/Ca and B/Ca. All of these elements may have some potential as palaeoenvironmental indicators in biogenic aragonites (Shen and Sanford, 1990, Beck et al., 1992, Mitsuguchi et al., 1996, Fallon et al. 1999). In addition, correlations between trace and minor elements have been used to infer controls in biogenic carbonate chemistry e.g. inverse correlations between Sr and Mg in deep sea corals may indicate Rayleigh fractionation (Gagnon et al., 2007) while trace element incorporation may be correlated with crystal growth rate in synthetic aragonites (e.g. Gabitov et al., 2008). We also made a preliminary suite of $\delta^{11}B$ analyses on this skeleton. The $\delta^{11}B$ of experimentally precipitated calcite and cultured foraminifera reflects the pH of local seawater (Sanyal et al., 1996, 2000) and the analysis of $\delta^{11}B$ in fossil foraminifera has been used to estimate past seawater pH (Sanyal et al., 1995). We estimate the likely pH of the fluids present during deposition of fused spherulites and epitaxial backfill.

2. Methods and materials

2.1. Sample preparation

We analysed an *A. willeyana* sponge (our reference NOM-1) collected from Nomuka Ika (174º49' W; 20º16′S), Tonga in November 2004. The specimen was found at a water depth of 9.5 m on the roof of a cave, under an overhang, on a modern coral reef framework. The sponge was collected from ~3.5 m into the cave. This cave had one large entrance (under the overhang) and several smaller conduits (from the back and sides of the cave) ensuring that is was well flushed with local sea water. The SST at the study site has an annual mean of 25.8 °C with a range of 4.3 °C, from ~24 °C (in August) to ~28 °C (in February/March) and we assume that this is reflective of water temperatures in the cave.

The sclerosponge was approximately hemi-spherical (with dimensions 34×20 mm) and was living when collected. After collection, the specimen was air-dried and returned to the UK for analysis. The sponge was sectioned along the axis of maximum vertical growth. One half of the sponge skeleton was divided into two and one of the resulting quarters was embedded in epoxy resin, mounted onto a 2.5 cm diameter glass slide and ground to a thickness of ~50 μm (Fig. 1) using silicon carbide papers and 0.3 μm polishing alumina lubricated with water.

2.2. SIMS

All analyses were made using a Cameca ims-4f ion microprobe in the School of GeoSciences at the University of Edinburgh. The section was gold coated and analysed with a $^{16}O^-$ beam, accelerated at 15 kV. Trace and minor element ratios were determined using 2 sets of instrument conditions. Instrument conditions, isotopes studied and typical count rates are summarised in Table 1. Annual cycles in trace/minor element composition were not obvious in preliminary analyses made using trace element conditions 1. Consequently the instrument conditions were adjusted, resulting in a smaller primary beam diameter and a higher analytical spatial resolution (trace element conditions 2). We estimate no significant isobaric interference for any of the isotopes studied (Allison 1996; Allison et al., 2007). Background counts were determined at mass 4.7 and were insignificant (<0.1 cps).

Trace element data were collected over two days and relative ion yields (RIY) for Mg/Ca, Sr/Ca and Ba/Ca were calculated from multiple analyses on the carbonate standard, OKA carbonatite (Mg/Ca = ~2.75 mmol mol^{-1}; Sr/Ca = ~13.66 mmol mol^{-1}; Ba/Ca = ~0.95 μmol mol^{-1}, see Allison et al., 2007). Instrument drift was insignificant over the 2 days. The accuracy of our SIMS estimates is affected by uncertainty in the composition of the standard (e.g. reflecting variations in the different OKA crystals used for SIMS and characterised by bulk analytical methods) and by potential matrix effects resulting from chemical and physical differences between the standard and samples, i.e. calcite and aragonite. To reduce this uncertainty, we have compared estimates of Mg/Ca, Sr/Ca and Ba/Ca along adjacent coral transects by SIMS and by bulk methods of analysis and calculated standardisation factors to apply to SIMS data (Allison et al., 2007). We have normalised all the SIMS data presented here using these factors. A relative ion yield for B/Ca was calculated from multiple analyses on the fasciculi of a *Porites* coral standard (M93-TB-FC-1, B/Ca = 0.36 mmol mol^{-1}, Kasemann et al., 2009).

Internal reproducibility (the precision at a single point) was calculated from the standard deviation (σ) of all cycles (n = number of cycles) in each sclerosponge analysis as ($\sigma/(\sqrt{n})$) and was typically 3%, 1.5%, <0.4% and 3% for B/Ca, Mg/Ca, Sr/Ca and Ba/Ca respectively, for

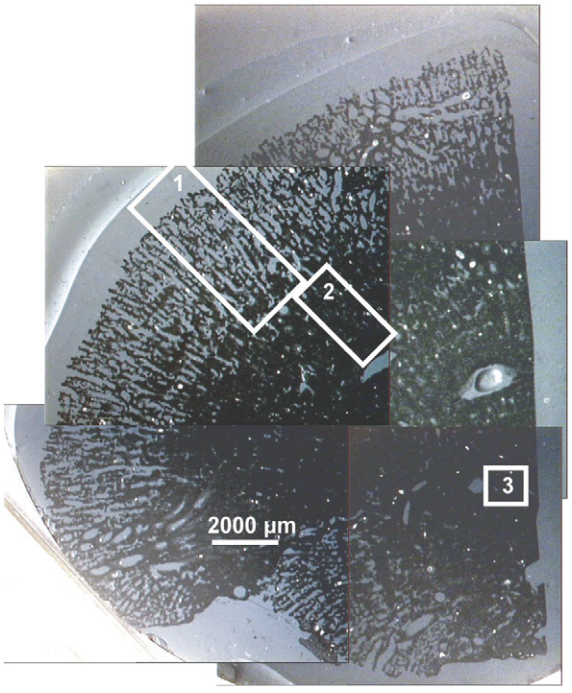

Fig. 1. Transmitted light micrograph of the sclerosponge section. The areas denoted by 1, 2 and 3 indicate the regions analysed for the spherulite transect, the epitaxial backfill and the spherulites at the centre of the skeleton, respectively.

Table 1
SIMS instrument conditions, isotopes studied and typical count rates (from analyses on sclerosponge). na = not analysed.

	Trace elements 1		Trace elements 2		$\delta^{11}B$	
Energy offset (V)	75		75		0	
Primary beam current (nA)	30		10		40	
Maximum beam diameter (μm)	20		15		35	
Imaged field (μm)	25		25		50	
Field aperture	2		1		1	
Contrast aperture	2		2		2	
Sample preclean	2 min with 50 μm raster		1 min in spot mode		1 min in spot mode	
Count times (per cycle) and count rates (cps):	Count time (s)	Count rate	Count time (s)	Count rate	Count time (s)	Count rate
^{10}B	na	–	na	–	5	700
^{11}B	8	160	na	–	3	2800
^{26}Mg	3	280	3	550	na	–
^{44}Ca	2	1.8×10^5	2	2.9×10^5	na	–
^{88}Sr	2	7.3×10^4	2	1.3×10^5	na	–
^{138}Ba	5	17	5	51	na	–
Number of cycles per analysis	10 or 15		10		100	

analyses of 10 cycles, and better than this for longer analyses. External reproducibility (the precision of 9 analyses on the OKA standard) was 0.4%, 0.5% and 0.8% for Mg/Ca, Sr/Ca and Ba/Ca respectively. External B/Ca reproducibility (the precision of 9 analyses on the coral standard) was 3%.

Sclerosponges are composed of two principle features: fused aragonitic spherulites and epitaxial backfill. After sample preparation the surface of the thin section associated with epitaxial backfilled areas achieved a smooth polish while aragonitic spherulites frequently appeared roughened. The centres of the spherulites are often mineralised incompletely (Worheide, 1998), leading to small voids in the section which may serve as traps for particulate materials and polishing compounds during sample preparation. We developed a protocol to screen out any contaminated analyses from the dataset. Ion count rates are typically constant or show small decreases over the course of an analysis on a carbonate material (Fig. 2a). The proportionate decrease may vary between isotopes and consequently, isotope/^{44}Ca ratios may subtly decrease or increase over longer analyses (Fig. 2b). Similar profiles of isotope/Ca behaviour are observed on carbonates of very different isotope/Ca composition. We compared the profiles of analyses on the sclerosponge (Mg/Ca = ~0.8 mmol mol^{-1}; Sr/Ca = ~11 mmol mol^{-1}; B/Ca = ~0.2 mmol mol^{-1}; Ba/Ca = ~4 μmol mol^{-1}), OKA carbonatite (Mg/Ca = ~3 mmol mol^{-1}; Sr/Ca = ~14 mmol mol^{-1}; Ba/Ca = ~1 μmol mol^{-1}) and the coral standard M93-TB-FC-1 (Mg/Ca = ~4 mmol mol^{-1}; Sr/Ca = ~9 mmol mol^{-1}; B/Ca = ~0.36 mmol mol^{-1}; Ba/Ca = ~3 μmol mol^{-1}, estimated from comparison with OKA). ^{11}B counts on the OKA standard are typically <1cps, so B/Ca profiles could only be compared between the sclerosponge and the coral standard. We rejected sclerosponge analyses which exhibited different isotope/Ca profiles compared to these standards e.g. some analyses exhibited much steeper B/Ca slopes, consistent with surface contamination of B. 43% of B/Ca and 35% of Ba/Ca analyses were rejected.

Instrument conditions for δ^{11}B analyses are summarised in Table 1. Secondary ions were collected using a mass resolution of ~800–900 and each analysis is the sum of 100 cycles. A pre-analysis sputter time of 1 min was used to remove surface contamination. The internal precision was typically 2.1‰. δ^{11}B was estimated by normalising the ^{11}B/^{10}B ratios of the coral sample to the mean ratio (3.784 ± 0.005 (1σ)) obtained from multiple SIMS analyses (n = 4) of a *Porites* coral standard (M93-TB-FC-1, δ^{11}B = 24.8 ± 0.4‰, 2σ, Kasemann et al., 2009).

We used SIMS to determine the geochemistry of selected areas of the sclerosponge. We made a series of trace/minor element analyses along a ~5 mm transect from the outermost surface of the skeleton towards the sponge centre (Fig. 1). Analyses were focused at the centres of the vertical skeletal pillars and examination of the section by transmitted light after analysis confirmed that all analyses were made on fused spherulites. Analyses were made along single pillars as much as possible. Additional analyses were made in the zone of epitaxial backfill and were focused on regions of epitaxial growth. Finally a small number of trace/minor element analyses (n = 10) were made on fused spherulites at the centre of the sponge, representing the oldest part of the skeleton (Fig. 1). 17 δ^{11}B analyses were made on the spherulites along the outermost 5 mm transect (region 1, Fig. 1). 24 δ^{11}B analyses were made at the centre of the sponge (region 3, Fig. 1), of these 9 were focused on fused spherulites and 15 on epitaxial backfill. The typical morphology of the different regions of the skeleton is illustrated in Fig. 3. SIMS analyses of the fused spherulites likely sample a mixture of intracellularly and extracellularly deposited aragonite i.e. the spherulites plus the fusing epitaxial growth. However it is difficult to estimate the proportions of these aragonites in each analysis. Mature spherulites have diameters of ~15 to ≥30 μm when released from the large vesicle cells (Worheide, 1998). The fused spherulites in this study have a typical diameter of ~20–30 μm (Fig. 4). During epitaxial fusing, the

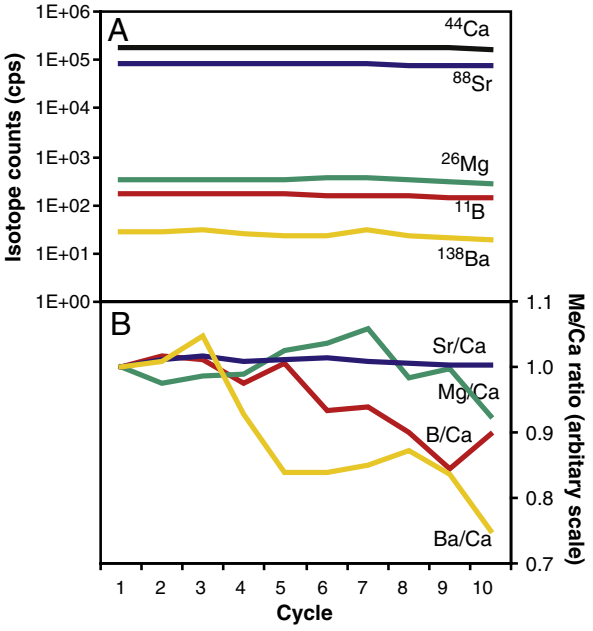

Fig. 2. A: Typical isotope counts rates and B: typical changes in Me/Ca ratios over 10 cycles on a sclerosponge analysis. In B, the Me/Ca ratio in the first cycle is scaled to 1.

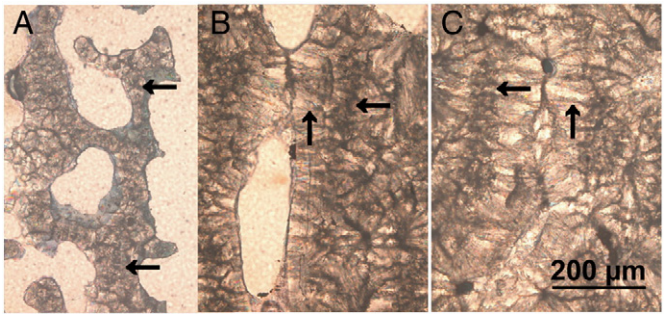

Fig. 3. Transmitted light micrographs of the sclerosponge skeleton, A: at the skeleton surface, B: ~4 mm from the surface and C: ~10 mm from the surface. Fused aragonitic spherulites are marked with horizontal arrows (←) in each image. Epitaxial backfill is marked with vertical arrows (↑) in B and C.

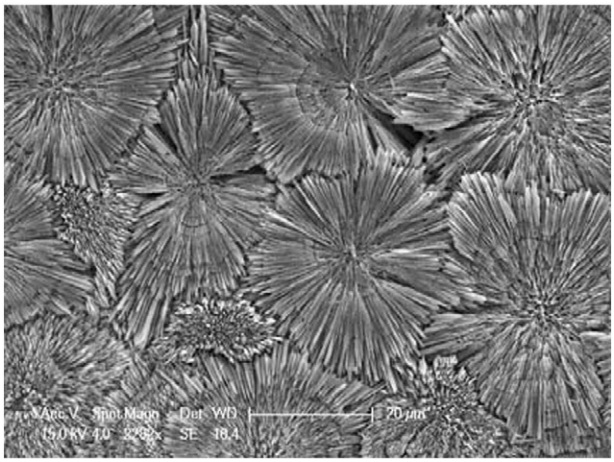

Fig. 4. Scanning electron micrograph of a broken cross-section of the sclerosponge skeleton showing the typical diameter of spherulites in the skeleton.

spherulite fibres extend in the direction of the c-axis of the aragonite crystal until they attain contact with fibres of other spherulites which prevent further extension (Worheide 1998). As a result many spherulites develop an asymmetrical shape. For simplicity, if we assume that the spherulites approximate the shape of a sphere and that their diameter is increased from 20 to 25 µm by epitaxial fusing, then we estimate that ~50% of the skeletal volume in the fused spherulites is deposited intracellularly as spherulites and 50% is deposited as epitaxial fusing. If epitaxial fusing increases the mean diameter of the spherulites by >5 µm then the contribution of epitaxially deposited aragonite to the skeletal volume will be even greater. This rough calculation demonstrates that a substantial proportion of the fused spherulites are deposited as epitaxial growth.

3. Results and discussion

Details of all individual SIMS analyses are summarised in Electronic Appendices 1 (trace and minor elements) and 2 ($\delta^{11}B$).

3.1. Skeletal $\delta^{11}B$ and precipitation fluid pH

$\delta^{11}B$ data are summarised in Table 2. The precision of single analyses was relatively large (typically ±2.1‰) and we did not observe significant differences between analyses in each group. We also did not observe significant differences in the mean $\delta^{11}B$ of the different regions i.e. between spherulites at the outer edge and centre of the sponge and epitaxial infill. We estimate the pH (total scale) of the precipitating fluid from skeletal $\delta^{11}B$ using the theoretical equation of B speciation in seawater (with boric acid $pK_B = 8.59$ (DOE 1994) at salinity = 35 and T = 26 °C, the mean seawater temperature at the study site). We use the empirically-determined boron isotope exchange equilibrium constant ($^{11-10}K_B$) in seawater of 1.0272 (Klochko et al., 2006) and assume that the $\delta^{11}B$ of the precipitation fluid is the same as seawater ($\delta^{11}B_{seawater} = 39.5‰$). The accuracy of our pH estimates is affected by the uncertainty in the $\delta^{11}B$ composition of the coral standard. Thermal ionisation and multi-collector inductively coupled plasma mass spectrometry analyses of 3 fragments of the same coral skeleton yielded $\delta^{11}B = 24.8 \pm 0.4‰$ (2σ, Kasemann et al., 2009), equivalent to a pH error ± ~0.03. However SIMS indicates that *Porites* corals are extremely heterogeneous with respect to $\delta^{11}B$ (Allison et al., 2010) and the thin section of the coral standard, cut parallel to the coral surface and representing a narrow time frame, may fall outside these limits. For this reason there may be a larger error in the accuracy of our pH estimates although the pattern of estimated pH variations is correct. We note that the mean $\delta^{11}B$ of a *Porites* coral (25.2 ± 1.8‰, 1σ, equivalent to pH 8.58), analysed by SIMS using the same standard, is in reasonable agreement (within 0.15 pH units) with the mean $\delta^{11}B$ estimated from other *Porites* corals (Honisch et al., 2004).

Table 2
Summary of skeletal $\delta^{11}B$ data and the estimated pH (total scale) of the precipitating fluid. 95% confidence intervals (ci) were calculated as $2^*\sigma/\sqrt{n}$.

Sample		$\delta^{11}B$			pH		
	n	Mean	σ	95% ci	Mean	σ	95% ci
Spherulites, region 1	17	20.3	1.8	0.9	8.24	0.13	0.07
Spherulites, region 3	9	18.7	2.7	1.8	8.08	0.26	0.17
Epitaxial infill, region 3	15	20.0	2.5	1.3	8.21	0.20	0.10

Our data suggest that the pH of the precipitating fluid is similar for the fused spherulites and the epitaxial backfill (Table 2). The pH of the fluid used for precipitation of sclerosponge skeletons is ~0.4–0.5 units lower than that of zooxanthellate corals and our tentative calibration suggests that the sclerosponge fluid has a similar pH to ambient seawater. The fluid used for extracellular precipitation, both epitaxial fusing and epitaxial backfill, is likely to be seawater. The origin of the fluid used for the intracellular precipitation of spherulites is unknown, but given the pH similarity, may also be based on seawater. In zooxanthellate corals, H^+ is extruded from the calcification fluid by the enzyme Ca-ATPase (Al Horani et al., 2003). The subsequent pH increase favours the conversion of $CO_2 \rightarrow HCO_3^- \rightarrow CO_3^-$, and facilitates the diffusion of CO_2 from the coral tissue into the calcification fluid. This results in high $CaCO_3$ supersaturation states and likely promotes rapid calcification (McConnaughey, 1989). Our data suggest that this mechanism does not operate in sclerosponges. A recent study suggests that a carbonic anhydrase may catalyse the conversion of $CO_2 \rightarrow HCO_3^- \rightarrow CO_3^-$ in the precipitation fluid contained in the large vesicle cells, increasing the fluid saturation state (Jackson et al., 2007).

Our estimates of precipitation fluid pH have several consequences. If sclerosponges skeletons record ambient seawater pH then fossil specimens may provide better indications of past seawater pH than other organisms which mediate the pH of their calcification fluids e.g. zooxanthellate corals (Al Horani et al., 2003) or calcitic foraminifera (de Nooijer et al. 2009). Sclerosponges may also be more susceptible to the effects of decreases in seawater pH if they do not have the ability to increase the pH of their precipitation fluids in response to ocean acidification.

We find no evidence that the pH of the precipitating fluid used to deposit the fused spherulites has changed significantly over the span of the sclerosponge life. $\delta^{11}B$ measurements in the outer transect of the skeleton were made from 0.6 to 3.4 mm from the skeleton surface. If we assume skeletal growth rates of 0.1–0.5 mm $year^{-1}$ (as suggested by the minimum and maximum periodicity of Sr/Ca and Mg/Ca variations, section 3.2), then we estimate that the analyses at the centre of the skeleton were deposited between 20 and 100 years before the analyses in the outer transect. The pH of the surface oceans was ~0.1 units higher in pre-industrial times compared to the present day (Caldeira and Wickett, 2003). We are unlikely to resolve this difference in our dataset, even if the sclerosponge skeleton is old enough to record it, as the precision of multiple (n = 9–17) $\delta^{11}B$ derived pH estimates is ±0.07–0.17 pH units (Table 2).

3.2. Cyclical trace/minor element variations

Sr/Ca, Mg/Ca and Ba/Ca variations across the fused spherulites transect from ~0 to 5 mm from the skeleton surface are illustrated in Fig. 5. Cyclical variations were not obvious in the outermost part of the transect i.e. in sections 1–3 from 0 to 2.4 mm from the skeleton surface. However, cyclical variations are apparent in both Sr/Ca and Mg/Ca in sections 4 and 5 of the transect (from 2.4 to 4.8 mm from the skeleton surface). The length of the cycles varies from ~0.1 mm

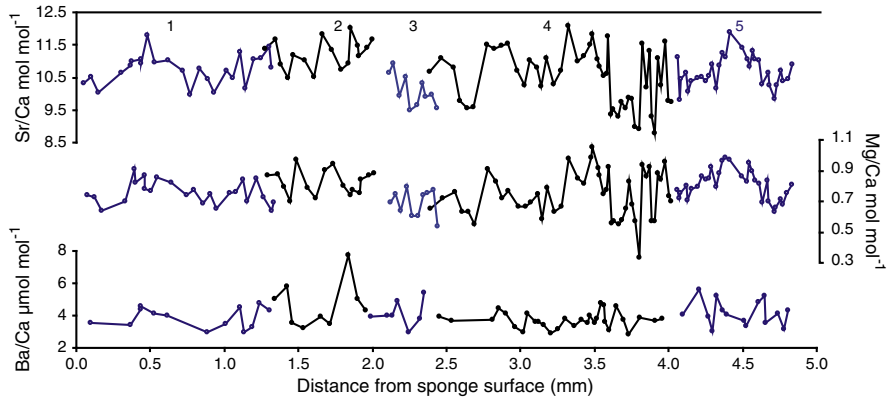

Fig. 5. Sr/Ca, Mg/Ca and Ba/Ca variations across the spherulite transect. Analyses were made along the single pillars, orientated perpendicular to the skeletal surface, as much as possible. Changes in pillar are denoted by the section numbers along the top of the graph and by breaks in the lines joining adjacent points. Precision of individual analyses (1σ) is smaller than the symbols in each case.

(i.e. from 3.8 to 4.0 mm) to ~0.4–0.6 mm (e.g. from 3.2 to 3.7 mm). Skeletal Ba/Ca does not follow any obvious cyclical pattern. Few credible B/Ca analyses were made along this transect using instrument conditions 1 and B was not analysed in instrument conditions 2 (Table 1). For this reason B/Ca variations are not illustrated.

Sclerosponge skeletons do not contain annual density band patterns and skeletal extension rates must be estimated by staining or dating skeletons. Estimated growth rates of *A. willeyana* skeletons range from ~0.2 mm yr^{-1} (Worheide, 1998) to 1.8 mm yr^{-1} (Fallon and Guilderson, 2005) at the Great Barrier Reef and from 0.4 to 0.7 mm yr^{-1} (Soloman Islands and Indonesian seaway, Moore et al., 2000) to ~1.6 mm yr^{-1} (Saipan, Northern Mariana Islands, Grottoli et al., 2010) in the tropical Western Pacific. Extension rates may vary by a factor of more than 2 within a single specimen (Fallon and Guilderson, 2005) or between individuals at the same location (Grottoli et al., 2010).It is therefore credible that some or all of the geochemical cycles reflect an annual seasonality. However, obvious cycles are not observed in the outermost part of the transect. Some of the observed cycles are short (~0.1 mm) and if the linear extension rate of the skeleton had slowed in the outermost section of the sclerosponge, then our sampling resolution may not be high enough to detect any annual cycles. This is particularly true for sections 1 and 2 of the transect which were analysed with a larger primary beam diameter compared to some other sections of the transect (see Appendix 1). In addition any annual cyclicity may be obscured if the sequential positions of the analyses do not directly reflect the timing of their deposition e.g. if some spherulites are deposited some distance into the tissue layer, rather than directly at the skeleton surface.

We have not plotted the analyses on the epitaxial backfill as a time series as it is difficult to constrain accurately the order in which the analysed regions were deposited. Similarly, we did not assign relative ages to the analyses made on the fused spherulites at the centre of the sponge. These analyses were made on multiple pillars within a small area and it was not possible to ascertain the order in which these regions had been deposited.

3.2.1. The inferred temperature sensitivity of Sr/Ca and Mg/Ca in fused spherulites

The observed Sr/Ca range in the fused spherulites is ~9.5 to 11.5 mmol mol^{-1}. The seawater temperature range at the study site is 4.3 °C and the skeletal Sr/Ca range is equivalent to a temperature sensitivity of ~0.5 mmol mol^{-1} °C (or ~5%°C^{-1}) assuming that the observed cycles are annual. This is in agreement with an *A. willeyana* specimen from Federated States of Micronesia (0.47 mmol mol^{-1} °C, Fallon et al., 2005) but considerably higher than estimates from other *A. willeyana* (0.12–0.17 mmol mol^{-1} °C, at the GBR, Fallon et al., 2005) or from *C. nicholsoni* (0.11 mmol mol^{-1} °C, Bahamas, Rosenheim et al., 2004). These previous sclerosponge calibration studies use LA-ICP-MS to sample backfilled skeletons and single analyses combine mixtures of fused spherulites and epitaxial backfill of significantly different ages, smoothing any encoded temperature signal. In light of this, it is not surprising that we observe a higher inferred temperature sensitivity than most other studies. The inferred temperature sensitivities for both Sr/Ca (~5%°C^{-1}) and Mg/Ca (~13%°C^{-1}) in our specimen (and in all other sclerosponge studies) are higher than observed in synthetically precipitated aragonites (~0.7%°C^{-1} for Sr/Ca and ~2%°C^{-1} for Mg/Ca, Gaetani and Cohen, 2006), indicating that the skeletal chemistry is also affected by other processes.

3.3. Correlations between trace/minor elements

To investigate the likely processes controlling trace/minor element incorporation, we plotted regressions between all the analysed trace/minor elements. For our plots we divided the dataset into 4 groups: the section of the fused spherulites transect which exhibited Sr/Ca and Mg/Ca cycles (i.e. sections 4 and 5, Fig. 5), the section of the transect which did not exhibit obvious cycles (i.e. sections 1 to 3, Fig. 5), the analyses of epitaxial backfill and the analyses on fused spherulites at the centre of the skeleton. We observed positive correlations between Sr and Mg in all the dataset groups (Fig. 6). The regression coefficient increased from 0.45, in the section of the transect which did not exhibit obvious cycles, to 0.87, in the analyses of spherulites at the centre of the skeleton (Table 3). We used regression analysis to test for differences in the regression equations of the four groups. Equations to describe the regressions between Sr/Ca and Mg/Ca in the different dataset groups, were not significantly different. The regression equation for the entire dataset is:

$$\mathrm{Sr/Ca}\left(\mathrm{mmol\ mol^{-1}}\right) = 4.60 * \mathrm{Mg/Ca}\left(\mathrm{mmol\ mol^{-1}}\right) + 7.13\left(r^2 = 0.64\right).$$

Ba and Sr (and Ba and Mg) were positively correlated in the epitaxial backfill and in the spherulites at the centre of the skeleton (Fig. 6, Table 3). They were not significantly correlated in the fused spherulites in the outer transect. We note that minimum Ba/Ca values in the outer transect fall along a Ba/Ca vs. Sr/Ca line which is similar to that describing the relationship in the epitaxial backfill and the spherulites at the sponge centre. We do not observe significant relationships between Sr/Ca and Ba/Ca in the outer transect, as many of the points contain higher Ba/Ca than is observed in the epitaxial backfill and the spherulites at the sponge centre. The mode of incorporation of Ba in the sclerosponge skeleton is unknown. In the outer transect

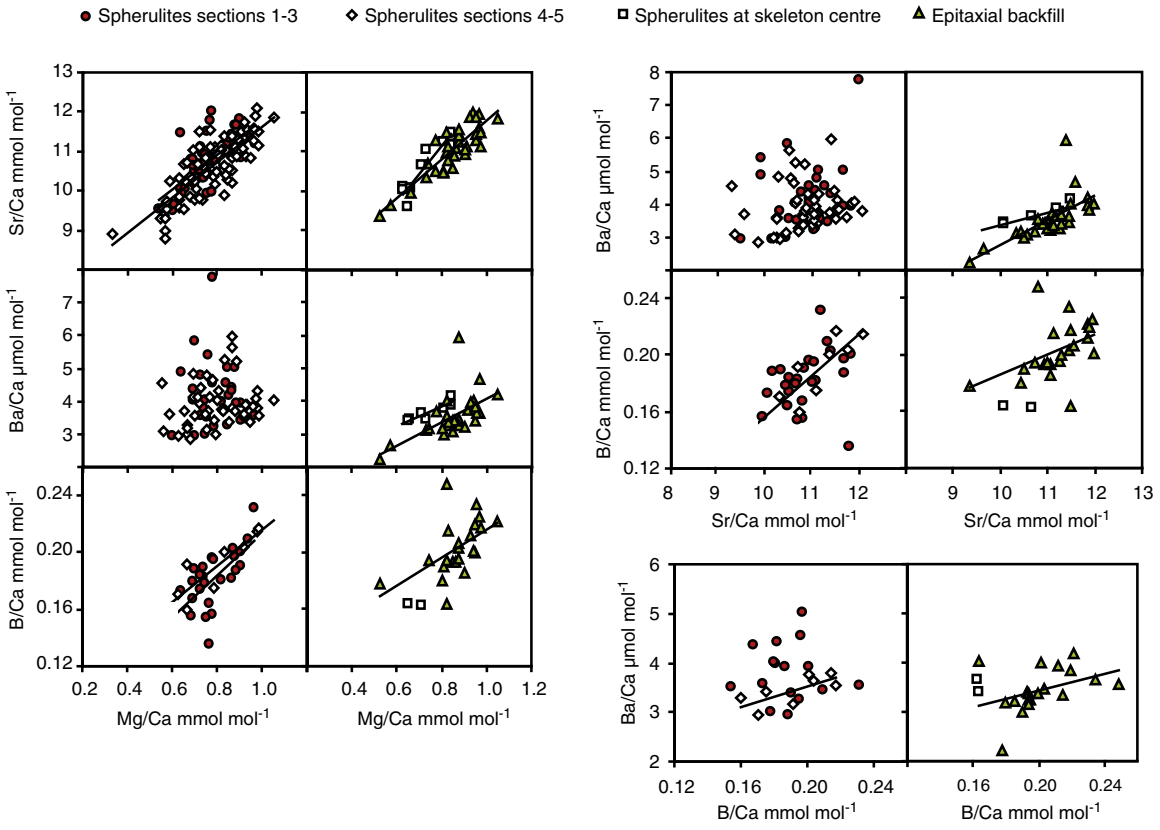

Fig. 6. Regressions between trace and minor elements in individual SIMS analyses. Black lines indicate linear correlations, where these are significant ($p = 0.05$). Precision of single analyses (1σ) is smaller than the symbols used in each case.

additional Ba may be incorporated in some non-lattice bound phase which decays through time, reducing the skeletal Ba/Ca to the typical range of values observed in the centre of the sponge. A similar mode of incorporation was suggested by Tudhope et al. (1996) to explain the high Ba/Ca observed in the outermost (most recently deposited) regions of massive *Porites* coral skeletons. We observed significant correlations of $r^2 > 0.5$ for B versus all other elements in sections 4 and 5 of the transect. In other regions of the skeleton, correlations between B and other elements were weaker or insignificant.

3.3.1. The role of Rayleigh fractionation

Rayleigh fractionation may occur when aragonite is precipitated from an isolated fluid reservoir. In the case of the sclerosponge this may be the fluid contained in the large vesicle cells which produce the spherulites or extracellular fluid trapped between the sponge tissue and the skeleton and used to produce epitaxial overgrowths. The Sr/Ca partition coefficient in aragonite is typically >1 (Gaetani and Cohen, 2006), so Sr is preferentially incorporated in the carbonate over Ca. As precipitation proceeds, the Sr/Ca of the fluid remaining in the reservoir, and of the aragonite subsequently precipitated from it, decrease. Conversely, the Mg/Ca partition coefficient in aragonite is <1 and the Mg/Ca of the remaining reservoir fluid, increases, as precipitation proceeds. The final Mg/Ca and Sr/Ca of the carbonate reflects the proportion of the reservoir used in precipitation (Elderfield et al., 1996). Rayleigh fractionation results in negative correlations between Mg/Ca and Sr/Ca in the precipitated aragonite. Our dataset demonstrates that Sr/Ca and Mg/Ca are positively correlated in all regions of the skeleton. This suggests that Rayleigh fractionation is not a significant control on the chemistry of the skeleton.

We note that the co-ordination of Mg and Sr in the sclerosponge skeleton is unknown. EXAFS studies of aragonitic coral skeletons and bivalve shells indicate that Sr substitutes in place of Ca in the carbonate lattice (Finch and Allison, 2003; Foster et al., 2009) while Mg is hosted by a disordered phase e.g. an organic component or nanoparticles of an inorganic phase (Finch and Allison, 2008; Foster et al., 2008). The co-ordination of Sr and Mg in different phases of the sclerosponge skeleton would invalidate this application of a Rayleigh model and it may be that either Sr or Mg is significantly controlled by Rayleigh fractionation. However our observation of strong positive correlations between Sr and Mg suggests that they are primarily controlled by a common factor.

Table 3
Correlation coefficients (r^2) of regressions between the trace element concentrations of individual SIMS analyses. ns = not significant. Insufficient credible B/Ca analyses were made on the spherulites at the centre of the sponge for regression analysis.

Series	Sr vs. Mg	Sr vs. Ba	Sr vs. B	Mg vs. Ba	Mg vs. B	Ba vs. B
Spherulite transect sections 1–3	0.45	ns	ns	ns	0.41	ns
Spherulite transect sections 4–5	0.66	ns	0.67	ns	0.76	0.54
Epitaxial infill	0.77	0.49	0.19	0.35	0.27	ns
Spherulites at centre of skeleton	0.87	0.65	–	0.79	–	–

3.4. Composition of different regions

We calculated the mean composition of the different skeletal regions (Fig. 7) and tested for difference between groups using ANOVA ($p = 0.05$). The Mg/Ca in the epitaxial backfill was significantly higher than in all the other groups. The Sr/Ca of the epitaxial backfill is significantly higher than that of the fused spherulites which exhibit cyclicity (but not significantly higher than that of the other spherulites) while the Ba/Ca of the backfill is significantly lower than that of the fused spherulites in regions 1–3. We did not observe any significant

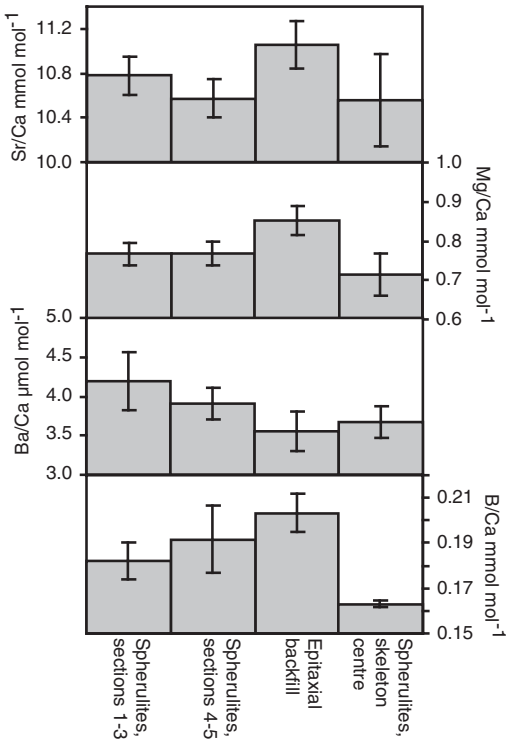

Fig. 7. Mean trace and minor element ratios of the different groups of the dataset. Bars show 95% confidence limits.

differences in the chemistry of the fused spherulites analysed in each group, with the exception that the spherulites at the centre of the sponge contained significantly less B/Ca than the spherulites, at or close to the sponge surface, and the epitaxial backfill.

We also combined all trace/minor element analyses on fused spherulites into one dataset and tested (*t*-test) for difference in the geochemistry of the fused spherulites and epitaxial backfill. Epitaxial backfill contained more Sr/Ca ($p = 0.002$), Mg/Ca ($p = 0.0001$) and B/Ca ($p = 0.0006$) and less Ba/Ca ($p = 0.01$) than the fused spherulites. The spherulites are deposited intracellularly while the epitaxial fusing and epitaxial backfill are deposited extracellularly. Differences in geochemistry between the features may reflect variations in the composition of the precipitation fluid, the incorporation of ions in the skeleton or kinetic effects e.g. crystal growth rate (Gabitov et al. 2008). We observe similar Sr/Ca and Mg/Ca ranges between the short and long length geochemical cycles in the fused spherulites (Fig. 5). If we assume that these cycles are annual, then the large variations in annual skeletal extension rate do not appear to affect the Sr/Ca and Mg/Ca of the skeleton. Little is known about crystal extension rates in sclerosponge skeletons. Spherulite formation begins with the deposition of 2–3 µm randomly orientated euhedral seed crystals. These crystals become radially orientated, extend as aragonite fibres and collectively grow to form round, egg-shaped or aster-shaped spherulites, which are typically ~15 µm in diameter. It is perhaps unlikely that skeletal extension and crystal extension rates are correlated i.e. during a slow growing year, fewer spherulites may be produced by the sponge, but each spherulite may be produced at a similar rate.

Both the vacuoles, in the large vesicle cells, and the extracellular spaces, from which epitaxial growth occurs, contain an acidic mucus with a large Ca^{2+} binding capacity (Worheide, 1998). However differences are observed in the organic matrix associated with the deposition of the spherulites, epitaxial fusing and epitaxial backfill. For example, the EDTA insoluble organic matrix in the extracellular spaces used to produce the epitaxial fusing is less dense than that observed in the large vesicle cells. The epitaxial backfill zone is characterised by a reduced number or absence of choanocytes (the flagellate cells responsible for inducing water currents inside the sponge) and symbiotic bacteria (Worheide, 1998). The spherulites contain the digested remains of symbiotic bacteria which may act as seeds for the nucleation of $CaCO_3$ (Jackson et al., 2010).

In spite of the variations in deposition environment between the fused spherulites and the epitaxial backfill we note that the mean pH of the depositional environments is similar and Sr/Ca and Mg/Ca are positively correlated by the same relationship in both fused spherulites and epitaxial backfill. This suggests that the geochemistry of each feature is predominantly controlled by a common process.

3.5. *A. willeyana* geochemistry as a palaeoenvironmental indicator

Our high spatial resolution SIMS record indicates that the presumably annual Sr/Ca variations in the fused spherulites transect are larger than observed in most other calibration studies which sample mixtures of fused spherulites and epitaxial backfill (Rosenheim et al., 2004; Fallon et al., 2005). The inferred temperature dependence of Sr/Ca is therefore higher, both from most other sclerosponges and from studies of synthetic aragonite (Gaetani and Cohen, 2006). This suggests that the chemistry of the *A. willeyana* skeleton is affected by one or more additional influences, which are currently unresolved.

This does not necessarily preclude the use of *A. willeyana* skeletons as indicators of sea surface temperature. The trace and minor element geochemistry of any biogenic aragonite is likely to represent a complex synthesis of influences including seawater temperature, crystal growth rate and biological effects. To be a successful indicator the skeletal structure must reliably reflect local environmental parameters. Fallon et al. (2005) observed a relatively poor ($r = \sim 0.5$) correlation between seawater temperature and seasonal Sr/Ca, in a LA-ICP-MS study of an *A. willeyana* skeleton. Single LA-ICP-MS analyses in the study combined mixtures of fused spherulites and epitaxial backfill which are deposited at substantially different times. An accurate seasonal SST signal may be recorded in the skeleton if the epitaxial backfill has a consistent composition and volume. Our data do not suggest that this is the case. We observe a large range in Sr/Ca (and Mg/Ca) in analyses on the epitaxial backfill, showing that its composition is as heterogeneous as that of the fused spherulites.

The epitaxial backfill, precipitated towards the base of the sponge calicle, has significantly different geochemistry, including higher Sr/Ca, compared to the fused spherulites, which are deposited at the skeleton surface. This observation emphasises the need to produce proxy calibrations from the basal (infilled) part of the skeleton. Samples from this part of the skeleton combine fused spherulites and epitaxial backfill and are analogous to skeletal samples produced from fossil specimens.

Supplementary materials related to this article can be found online at doi:10.1016/j.palaeo.2011.10.009

Acknowledgements

Access to the ion probe was provided by NERC Scientific Services and we thank Richard Hinton for his assistance with the analyses. We thank Mike Hall for making the section and Thierry Correge (Editor), Brad Rosenheim and another anonymous reviewer for constructive comments which improved this manuscript.

References

Al-Horani, F.A., Al-Moghrabi, S.M., de Beer, D., 2003. The mechanism of calcification and its relation to photosynthesis and respiration in the scleractinian coral *Galaxea fascicularis*. Marine Biology 142, 419–426.

Allison, N., 1996. Quantitative determinations of trace and minor elements in coral aragonite by ion microprobe analysis, with preliminary results from Phuket, South Thailand. Geochimica et Cosmochimica Acta 60, 3457–3470.

Allison, N., Finch, A.A., Webster, J.M., Clague, D.A., 2007. Palaeoenvironmental records from fossil corals: the effects of submarine diagenesis on temperature and climate estimates. Geochimica et Cosmochimica Acta 71, 4693–4703.

Allison, N., Finch, A.A., EIMF, 2010. δ11B, 2010. Sr, Mg and B in a modern Porites coral: the relationship between calcification site pH and skeletal chemistry. Geochimica et Cosmochimica Acta 74, 1790–1800.
Beck, J.W., Edwards, R.L., Ito, E., et al., 1992. Sea-surface temperature from coral skeletal strontium calcium ratios. Science 257, 644–647.
Böhm, F., Joachimski, M., Lehnert, H., Morgenroth, G., Kretschmer, W., Vacelet, J., Dullo, W.-C., 1996. Carbon isotope records from extant Caribbean and South Pacific sponges: Evolution of $\delta^{13}C$ in surface water DIC. Earth and Planetary Science Letters 139, 291–303.
Böhm, F., Haase-Schramm, A., Eisenhauer, A., Dullo, W.-C., Joachimski, M.M., Lehnert, H., Reitner, J., 2002. Evidence for preindustrial variations in the marine surface water carbonate system from coralline sponges. Geochemistry, Geophysics, Geosystems 3, 1019. doi:10.1029/2001GC000264.
Caldeira, K., Wickett, M.E., 2003. Anthropogenic carbon and ocean pH. Nature 425, 365.
D.O.E., 1994. Handbook of Methods for the Analysis of the Various Parameters of the Carbon Dioxide System in Seawater. In: Dickson, A.G., Goyet, C. (Eds.), ORNL/CDIAC-74, Version 2. Department of Energy.
de Nooijer, L.J., Toyofuku, T., Kitazato, H., 2009. Foraminifera promote calcification by elevating their intracellular pH. Proceedings of the National Academy of Science 106, 15374–15378.
Elderfield, H., Bertram, C.J., Erez, J., 1996. Biomineralization model for the incorporation of trace elements into foraminiferal calcium carbonate. Earth and Planetary Science Letters 142, 409–423.
Fallon, S.J., Guilderson, T.P., 2005. Extracting growth rates from the nonlaminated coralline sponge *Astrosclera willeyana* using bomb radiocarbon. Limnology and Oceanography Methods 3, 455–461.
Fallon, S.J., McCulloch, M.T., van Woesik, R., Sinclair, D.J., 1999. Corals at their latitudinal limits: laser ablation trace element systematics in Porites from Shirigai Bay, Japan. Earth and Planetary Science Letters 172, 221–238.
Fallon, S.J., McCulloch, M.T., Guilderson, T.P., 2005. Interpreting environmental signals from the coralline sponge *Astrosclera willeyana*. Palaeogeography, Palaeoclimatology, Palaeoecology 228, 58–69.
Finch, A.A., Allison, N., 2003. Strontium in coral aragonite: 2. Sr co-ordination and the long-term stability of environmental records. Geochimica et Cosmochimica Acta 67 (23), 4519–4527.
Finch, A.A., Allison, N., 2008. Mg structural state in coral aragonite and implications for the paleoenvironmental proxy. Geophysical Research Letters 35, L08704. doi:10.1029/2008GL033543.
Foster, L., Finch, A.A., Allison, N., Andersson, C., Clarke, L.J., 2008. Mg in aragonitic bivalve shells: seasonal variations and mode of incorporation in *Arctica islandica*. Chemical Geology 254, 113–119.
Foster, L.C., Allison, N., Finch, A.A., Andersson, C., 2009. Strontium distribution in the shell of the aragonite bivalve *Arctica islandica*. Geochemistry, Geophysics, Geosystems 10, Q03003. doi:10.1029/2007GC001915.
Gabitov, R.I., Gaetani, G.A., Watson, E.B., Cohen, A.L., Ehrlich, H.L., 2008. Experimental determination of growth rate effect on U6+ and Mg2+ partitioning between aragonite and fluid at elevated U6+ concentration. Geochimica et Cosmochimica Acta 72, 4058–4068.
Gaetani, G.A., Cohen, A.L., 2006. Element partitioning during precipitation of aragonite from seawater: a framework for understanding paleoproxies. Geochimica et Cosmochimica Acta 70, 4617–4634.
Gagnon, A.C., Adkins, J.F., Fernandez, D.P., Robinson, L.F., 2007. Sr/Ca and Mg/Ca vital effects correlated with skeletal architecture in a scleractinian deep-sea coral and the role of Rayleigh fractionation. Earth and Planetary Science Letters 261, 280–295.
Grottoli, A.G., Adkins, J.F., Panero, W.R., Reaman, D.M., Moots, K., 2010. Growth rates, stable oxygen isotopes ($\delta^{18}O$), and strontium (Sr/Ca) composition in two species of Pacific sclerosponges (*Acanthocheatetes wellsi* and *Astrosclera willeyana*) with $\delta^{18}O$ calibration and application to paleoceanography. Journal of Geophysical Research 115, C06008. doi:10.1029/2009JC005586.
Haase-Schramm, A., Böhm, F., Eisenhauer, A., Dullo, W.-C., Joachimski, M.M., Hansen, B., Reitner, J., 2003. Sr/Ca ratios and oxygen isotopes from sclerosponges: temperature history of the Caribbean mixed layer and thermocline during the Little Ice Age. Paleoceanography 18. doi:10.1029/2002PA000830.
Honisch, B., Hemming, N.G., Grottoli, A.G., Amat, A., Hanson, G.N., Bjima, J., 2004. Assessing scleractinian corals as recorders for paleo-pH: empirical calibration and vital effects. Geochimica et Cosmochimica Acta 68, 3675–3685.
Jackson, D.J., Macis, L., Reitner, J., Degnan, B.M., Woerheide, G., 2007. Sponge paleogenomics reveals an ancient role for carbonic anhydrase in skeletogenesis. Science 316, 1893–1895.
Jackson, D.J., Thiel, V., Woerheide, G., 2010. An evolutionary fast-track to biocalcification. Geobiology 8, 191–196.
Kasemann, S.A., Schmidt, D.N., Bijma, J., Foster, G.L., 2009. In situ boron isotope analysis in marine carbonates and it's application for foraminifera and palaeo-pH. Chemical Geology 260, 138–147.
Kinsman, D.J.J., Holland, H.D., 1969. The coprecipitation of cations with $CaCO_3$: IV. The coprecipitation of Sr^{2+} with aragonite between 16 and 96°C. Geochimica et Cosmochimica Acta 33, 1–17.
Klochko, K., Kaufman, A.J., Yao, W.S., Bryne, R.H., Tossell, J.A., 2006. Experimental measurement of boron isotope fractionation in seawater. Earth and Planetary Science Letters 248, 276–285.
McConnaughey, T.A., 1989. ^{13}C and ^{18}O isotopic disequilibrium in biological carbonates: II. In vitro simulation of kinetic isotope effects. Geochimica et Cosmochimica Acta 53, 163–171.
Mitsuguchi, T., Matsumoto, E., Abe, O., Uchida, T., Isdale, P.J., 1996. Mg/Ca thermometry in coral-skeletons. Science 274, 961–963.
Moore, M.D., Charles, C.D., Rubenstone, J.L., Fairbanks, R.G., 2000. U/Th-dated sclerosponges from the Indonesian Seaway record subsurface adjustments to west Pacific winds. Paleoceanography 15, 404–416.
Rosenheim, E.B., Swart, P.K., Thorrold, S.R., Willenz, P., Berry, L., Latkoczy, C., 2004. High-resolution Sr/Ca records in sclerosponges calibrated to temperature in situ. Geology 32, 145–148.
Rosenheim, B.E., Swart, P.K., Willenz, P., 2009. Calibration of sclerosponge oxygen isotope records to temperature using high-resolution $\delta^{18}O$ data. Geochimica et Cosmochimica Acta 73, 5308–5319.
Sanyal, A., Hemming, N.G., Hanson, G.N., Broecker, W.S., 1995. Evidence for a higher pH in the glacial ocean from boron isotopes in foraminifera. Nature 373, 234–236.
Sanyal, A., Hemming, N.G., Broecker, W.S., Lea, D.W., Spero, H.G., Hanson, G.N., 1996. Oceanic pH control on the boron isotopic composition of foraminifera: evidence from culture experiments. Paleoceanography 11, 513–517.
Sanyal, A., Nugent, M., Reeder, R.J., Bijima, J., 2000. Seawater pH control on the boron isotopic composition of calcite: evidence from inorganic calcite precipitation experiments. Geochimica et Cosmochimica Acta 64, 1551–1555.
Shen, G.T., Sanford, C.L., 1990. Trace element indicators of climate change in annually banded corals. In: Glynn, P.W. (Ed.), Global Ecological Consequences of the 1982–83 El Nino. Elsevier, New York, pp. 255–283.
Swart, P.K., Thorrold, S.R., Rosenheim, B.E., Eisenhauer, A., Harrison, C.G.A., Grammer, M., Latkoczy, C., 2002. Intra-annual variation in the stable oxygen and carbon and trace element composition of sclerosponges. Paleoceanography 17. doi:10.1029/2000PA000622.
Tudhope, A.W., Lea, D.W., Shimmield, G.B., Chilcott, C.P., Head, S., 1996. Monsoon climate and Arabian sea coastal upwelling recorded in massive corals from southern. Palaios 11, 347–361.
Worheide, G., 1998. The reef cave dwelling ultraconservative coralline demosponge Astrosclera willeyana (LISTER 1900) from the Indo-Pacific, micromorphology, ultrastructure, biocalcification, isotope record, taxonomy, biogeography, phylogeny. Facies 38, 1–88.